Check for updates

Magnetic Resonance Imaging and Ultrasonographic Evaluation of Canine Tarsus

Soomin Park
Sang-hwa Ryu
Jae-gwan Heo
Eun-jee Kim
Jihye Choi
Junghee Yoon*

College of Veterinary Medicine and the Research Institute for Veterinary Science, Seoul National University, Seoul 08826, Korea

*Correspondence: heeyoon@snu.ac.kr

ORCID
Soomin Park:
 https://orcid.org/0000-0002-1116-1091
Sang-hwa Ryu:
 https://orcid.org/0009-0008-3249-1242
Jae-gwan Heo:
 https://orcid.org/0009-0006-7083-0132
Eun-jee Kim:
 https://orcid.org/0009-0006-3613-7887
Jihye Choi:
 https://orcid.org/0000-0002-1258-7158
Junghee Yoon:
 https://orcid.org/0000-0002-2077-763X

Abstract The tarsus in dogs has a complex structure that makes its evaluation relatively challenging. Because an accurate diagnosis of the tarsus is difficult through basic examinations alone, imaging tests are essential. Previous studies have explored the anatomical and radiological features of the canine tarsus using several imaging modalities. However, the imaging utility of the tarsus across different modalities has not been thoroughly evaluated. This study aimed to visualize the tarsal structures using magnetic resonance imaging (MRI) and ultrasonography, compare their utility, and propose suitable imaging modalities and conditions for evaluating specific tarsal structures. Magnetic resonance imaging and ultrasound scans of the tarsus of four healthy dogs were performed, and two observers rated the utility of each image on a five-point scale. Although MRI is more beneficial for assessing the tarsal structures than ultrasound, ultrasound also appears clinically useful for evaluating the cranial tibialis muscle, deep digital flexor tendon, subcutaneous fat, joint space, and superficial digital flexor tendon. In addition, each structure of interest can be evaluated for optimal visibility using specific ultrasound sections, MRI sequences, and planes. In veterinary clinical practice, an initial assessment using ultrasound imaging with optimal visibility is required and if further evaluation is necessary, MRI examinations with optimal MRI sequences and planes can be performed.

Key words dog, tarsus, ultrasonography, magnetic resonance imaging.

Introduction

The tarsus is located between the tibia-fibula and the metatarsus (4,11). It comprises joints composed of seven tarsal bones surrounded by soft tissues, including joint capsules, tendons, blood vessels, and ligaments (1,11). Although the tarsal joint plays a role in shock absorption, it lacks sufficient support and protection from the surrounding soft tissues, making it susceptible to injuries (2). In addition, the tarsal joint can be affected by various developmental conditions (1). These pathologies may cause severe clinical issues when accompanied by complications (21,23,29). Representative conditions of the tarsus with clinical significance in dogs include Achilles tendon injuries, osteitis dissection, and fractures (24,29).

Through orthopedic examinations, tarsal pathologies can be localized; however, a thorough assessment based solely on physical examinations remains challenging (3). Additionally, while radiography serves as a readily accessible, noninvasive, and cost-effective imaging tool, it may limit the ability to achieve a clear evaluation and may not be sufficient for assessing the surrounding soft tissues (7). Employing stress views becomes arduous when multiple structures are affected, or when injuries are partial (3).

To overcome these limitations, evaluation of tarsal structures using several imaging modalities has been reported (3,7,10,11). Ultrasonography has been demonstrated to be effective in the diagnosis of soft tissue injuries in the tarsus (3,8). Computed tomography (CT) images offer comprehensive anatomical information on bony structures, tendons, and major blood vessels, providing valuable insights for evaluating tarsal joint injuries (11). Most soft tissue structures were identified using transverse magnetic resonance imaging (MRI) sections (7,20). Considering the previous literature, both MRI and ultrasonography are advantageous for assessing soft tissues, including tendons and ligaments (3,7).

Anatomical comparisons of the tarsal structure using cadavers and the assessment of image quality in specific pathologies are the only aspects reported in previous tarsal MRI studies (1,2,7,27). Ultrasonographic research has also been limited and has primarily focused on the visual representation of specific structures, scanning techniques, and images within a pathological environment (3,15,18). A comprehensive assessment of various structures within the tarsal region, including bones, muscles, tendons, and subcutaneous fat; the usefulness of evaluations; and the development of scan protocols for assessment have not yet been conducted in either modality (16).

The objectives of this study were to 1) evaluate the utility of assessing tarsal structures in both MRI and ultrasound by scoring, 2) determine the most valuable MRI sequence for tarsal evaluation, and 3) assess the most favorable planes and sequences for the evaluation of each tarsal structure in both modalities with the aim of facilitating clinical application.

Materials and Methods

Animals

Four adult male beagle dogs were used in this study, and eight tarsi were examined. The mean age was 5 years and the median weight was 15 kg (range, 12-17 kg). All dogs were confirmed healthy through physical examinations, complete blood count, serum biochemistry, blood pressure measurements, radiographic examinations, and ultrasound examinations. MRI (Sigma creator 1.5T; GE; USA) was the initial imaging modality, and ultrasonography was performed using a 12-MHz linear transducer (Arietta 850SE; Hitachi-Aloka; Japan). All imaging examinations were performed by a veterinarian (P.S.M) with 2 years of experience in imaging. The evaluated structures included the tarsal vessels, bone, joint spaces, subcutaneous fat, cranial tibial muscle, superficial digital flexor tendon, deep digital flexor tendon, and cranialis tibialis tendon.

This study was approved by the Institutional Animal Care and Use Committee of Seoul National University, and the dogs were cared for according to the guidelines for Animal Experiments of Seoul National University (SNU IACUC-230801-4).

Magnetic resonance imaging

After fasting the dog for at least 6 hours, sedation was induced by an intravenous injection of medetomidine (Domitor; Orion; Finland) at a dose of 0.01 mg/kg. After 15 min, general anesthesia was induced by intravenous injection of alfaxalone (Alfaxan; Jurox; Australia) at a dose of 3 mg/kg, and anesthesia was maintained with isoflurane (Ifran; Hana Pharm; South Korea) concentration of 2.0% and oxygen.

MRI was performed using a 1.5-Tesla whole-body scanner with a receive-only single-channel small-flex coil. The dog was placed in the lateral recumbent position and the ipsilateral tarsus was flexed at an angle of 140°. Images were acquired at a slice thickness of 2 mm and scanned from the distal fourth of the tibia to the proximal third of the metatarsus.

Localizer imaging was performed with three orthogonal planes using T1-weighted (T1W) three-dimensional turbo field echo scans. The transverse plane was aligned parallel to the tarsometatarsal joint, the sagittal plane was aligned parallel to the sagittal plane of the calcaneus, and the dorsal plane was set perpendicular to both the sagittal and trans-

verse planes for imaging (7). Subsequently, the dorsal, transverse, and sagittal planes were obtained using T2-weighted (T2W), T1W, and proton density with fat saturation (PD FS) sequences. Each sequence was acquired using the following parameters: T2W ([repetition time (TR)]: 3876 ms, [echo time (TE)], 66 ms), T1W ([TR]: 682 ms; [TE]: 11 ms), and PD FS ([TR]: 2200 ms, [TE]: 36 ms). The field of view was 10 × 10 cm in the dorsal and sagittal planes and 14 × 14 cm in the transverse plane. The scan time for each tarsus was 90 min. After the MRI scans, oxygen was supplied, and the dogs were monitored for 1 h until recovery. All MRI images were transferred to a PACS System (INFINITT PACS; Infinitt Healthcare; South Korea).

Ultrasonography

Prior to ultrasound, the hair was clipped from the midtibia to the level of the metatarsophalangeal joint. Ultrasonography was performed using a 12-MHz linear transducer. The scans were performed in the following sequence: dorsal, plantar, lateral, and medial. The dog was positioned in dorsal recumbency for the dorsal and plantar portions of the tarsus, right lateral recumbency for the right medial and left lateral portions, and left lateral recumbency for the left medial and medial portions of the tarsus. During scanning, the probe was moved from the proximal to distal aspect and from the medial to lateral aspect.

Image analysis

The assessment was conducted based on the degree of structural visualization and scoring was conducted separately for each structure. Utility was rated on a 5-point scale: 1 = not assessable at all, 2 = minimally assessable with low reliability, 3 = partially assessable with moderate reliability, 4 =

mostly assessable with high reliability but not entirely, and 5 = fully assessable with high reliability. Identical evaluation criteria were provided to the observers and the results were not shared (Fig. 1).

All MRI images were transferred and assessed on a PACS System Elva by two veterinarians (P. S. M. and R. S. H.), both with 2 years of radiology experience. The MRI images were simultaneously presented, and the evaluation order of the structures was random. Assessment was conducted using three sequences, including T1W, T2W, and PD FS on MRI, and the evaluations were conducted in the sagittal, dorsal, and transverse planes.

Ultrasonography was performed by one veterinarian (P.S.M) and concurrently assessed by the same two observers evaluated the MRI images. The evaluation was conducted anatomically at positions that could best scan the respective structures. The scanning sequence was conducted in the following order: dorsal, plantar, lateral, and medial approaches. The bone, cranial tibial muscle, cranialis tibialis tendon, and joint space were scanned using a dorsal approach, whereas the superficial and deep digital flexor tendons were examined using a plantar approach. In the lateral approach, the examination included the bone, subcutaneous fat, and vascular structures, whereas in the medial approach, the bone and subcutaneous fat were scanned. Scans were conducted in both the transverse and longitudinal views.

Statistical analyses

Statistical analyses were conducted to determine the most useful MRI sequence for tarsal evaluation, recommend the preferred sequence and plane for evaluating each structure during MRI assessments, identify structures that can be evaluated using ultrasound, and specify the optimal approach

Fig. 1. Representative magnetic resonance imaging images corresponding to evaluation criteria scores in utility assessment. Transverse T2-weighted image (a), sagittal T1-weighted image (b), and dorsal proton density fat saturation image (c) of the canine tarsus. The joint space (long arrow) received a score of 2, the bone (asterisk) was rated at 5 in (a), blood vessels (arrowhead) were assigned 4 points, the cranialis tibialis tendon (short arrow) scored 3 points in (b), and the cranial tibial muscle (dashed arrow) was assessed with 1 in (c).

and view for ultrasound examination.

Statistical analyses were performed by one author (P. J. Y.) using commercially available software (IBM SPSS Statistics 27.0; IBM Corporation; USA). Interobserver agreements were assessed using the interclass correlation coefficient (ICC) test: ICC < 0.4 (poor agreement), ICC 0.41-0.6 (moderate agreement), ICC 0.61-0.8 (good agreement), ICC > 0.8 (excellent agreement) (22).

Results

The score is evaluated by averaging the scores given by two observers. In the MRI assessment, various structures were evaluated in different sequences and cross-sectional planes, including transverse, dorsal, and sagittal sections. When considering the overall scores, the average scores were as follows: T1W scored 3.72, T2W scored 3.59, and PD FS scored 2.69 (Fig. 2, Table 1).

In the comprehensive evaluation of structures using MRI, the sequences and planes that are considered most favorable for evaluating each structure are as follows: the bone structures received an average score above 3.0 in most plane in T1W, T2W, and PD FS. Subcutaneous fat evaluation yielded an average score of 4.5 in the specific plane of T1W and T2W, whereas PD FS scored under 3.0 in all planes. The vascular structures and cranial tibialis muscle both received the highest score of 4.5 in the sagittal plane of T1W sequence. Joint space received a highest score of 4.0 in the dorsal and sagittal planes in both T1W and T2W sequences. Both the superficial digital flexor tendon and deep digital flexor tendon received their highest scores in sagittal plane. Finally, although the cranialis tibialis tendon scored the highest, with 3.25 in the transverse plane of T1W, it received under 3.0 in the other sequences and planes (Fig. 3).

The assessment of the bone structures involved the dorsal approach, and the average score was 1.0 across all views. Subcutaneous fat in the dorsal approach received a score above 3.0, whereas vascular structures received scores under
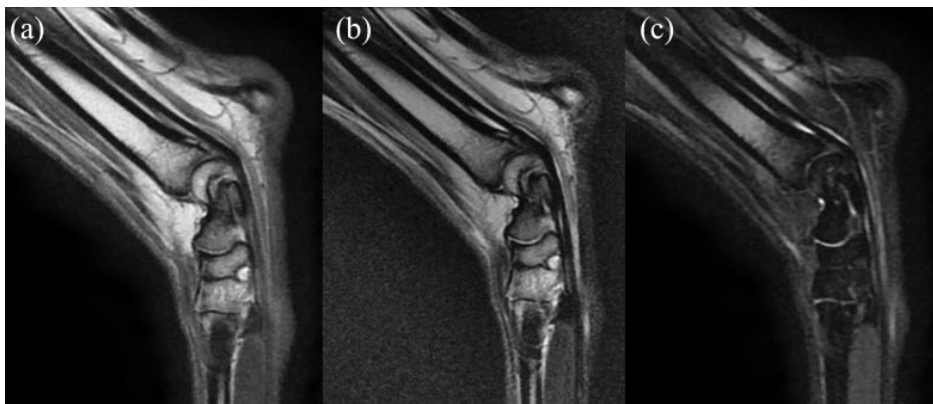

Fig. 2. The appearance of each tarsus on magnetic resonance imaging sequences. Sagittal T1-weighted image (a), T2-weighted image (b) and proton density fat saturation image (c) of the lateral region of the canine tarsus. T1W was rated as the most useful with a score of 3.72 for the overall evaluation of tarsal structures, followed by T2W at 3.59, and PD FS at 2.69.

Table 1 The mean score based on sequences and planes for each structure in MRI

Evaluation factors	T1W			T2W			PD FS		
	Sagittal	Dorsal	Trans	Sagittal	Dorsal	Trans	Sagittal	Dorsal	Trans
Bone	4.50	4.00	4.50	4.25	3.75	4.25	3.00	2.75	3.00
Subcutaneous fat	4.50	3.75	4.50	4.50	3.50	4.50	2.25	2.00	2.50
Vascular structure	4.00	2.75	3.50	3.25	2.50	3.50	3.25	2.00	3.25
Joint space	4.00	4.00	2.00	4.00	4.00	2.00	3.75	3.50	1.25
Cranial tibial muscle	4.50	3.75	4.00	4.25	4.00	4.00	3.00	2.50	3.00
CTT	3.00	2.50	3.25	2.75	2.50	2.75	2.25	1.50	2.00
SDFT	4.25	3.25	3.75	4.25	3.25	3.25	3.25	2.50	3.00
DDFT	4.25	3.25	3.75	4.25	3.50	3.50	3.50	2.50	3.00

CTT, cranialis tibialis tendon; SDFT, superficial digital flexor tendon; DDFT, deep digital flexor tendon.

Fig. 3. T1-weighted (a-c), T2-weighted (d-f), and proton density fat saturation (g-i) images of the tarsal structures evaluated with a score above 3.0.; short arrow, cranialis tibialis tendon; dashed arrow, joint space; black arrow, vascular structure; asterisk, bone; arrowhead, cranial tibial muscle; long arrow, superficial and deep digital flexor tendons.

3.0. Cranial tibial muscle was rated at 3.75 in both views, while joint space scored under 3.0 in the transverse view and 3.0 in the longitudinal view. The cranialis tibialis tendon scored under 3.0 in all cases. The deep and superficial digital flexor tendons were assessed using a plantar approach. The former received scores of 3.25 and 3.75, whereas the latter scored 2.5 and 3.0 in the transverse and longitudinal views, respectively (Table 2, Fig. 4).

The study observed ICC values in the order of sagittal, dorsal, and transverse planes for the PD FS, T1W, and T2W MRI sequences, which were as values for PD FS MRI were 0.796, 0.854, and 0.853, respectively. The T1W MRI values were 0.739, 0.771, and 0.882, respectively. The T2W MRI values were 0.723, 0.749, and 0.791, respectively. Ultrasound exhibited ICC values of 0.916 and 0.880 in the longitudinal and transverse views, respectively. These ICC values quantify the level of agreement or reliability in image assessments across different planes and sequences for MRI as well as views for ultrasound.

Discussion

The evaluated structures were selected on the basis of previous reports. The tarsus is composed of various bones, and fractures and bone tumors have been reported; therefore, bone assessment was included (9). In the case of blood vessels, reports of hindlimb angiomatosis were considered (14). Specifically, the assessment focused on the saphenous lateral vein, which is a size that allows for ultrasound evaluation (19). Luxation and arthritis of the tarsal joints, along with reported tumors such as synovial cell sarcoma, prompted the inclusion of joint space in the evaluation of the structure (5). In this study, evaluation of the tibiotarsal joint, which is the most easily locatable joint during ultrasound and controls 80% of

Table 2 The mean score for each structure in ultrasound on transverse and longitudinal views

Evaluation factors	Transverse view	Longitudinal view
Bone	1.00	1.00
Subcutaneous fat	3.25	3.25
Vascular structure	2.25	1.25
Joint space	2.75	3.00
Cranial tibial muscle	3.75	3.75
CTT	2.75	2.50
SDFT	2.50	3.00
DDFT	3.25	3.75

CTT, cranialis tibialis tendon; SDFT, superficial digital flexor tendon; DDFT, deep digital flexor tendon.

the range of motion of the tarsus, was particularly focused (12). Regarding subcutaneous fat, although there have been no reported cases in the tarsal area, evaluations were conducted together owing to reports of lipoma and subcutaneous mass occurrence in the hind limb (28). Although the tarsal region lacks muscles, one study suggested the surgical use of a fascia graft from the cranial tibial muscle in cases of tarsal tendon damage (6,25). Consequently, both the associated muscles and connected tendons were added as evaluation structures. Trauma-induced tendon rupture is relatively common, and damage to the ligaments and tendons in the plantar area has been identified as a potential cause of calcaneoquartal and tarsometatarsal instability (12). Therefore, this study evaluated two digital flexor tendons located in the plantar area that can be visualized using ultrasound (3). Although collateral ligament damage can be a contributing factor, it was not included as an evaluation criterion because of potential challenges in ultrasound imaging, as elucidated in previous studies (3,26).

In this study, T2W, T1W, and PD FS sequences were examined using MRI. The rationale for selecting these sequences was based on previous reports concerning MRI assessment of the extremities, such as the tarsus or carpus (7,10,17,21). Although the T2W sequence has limitations in visualizing anatomical structures, it is useful for detecting artifacts stemming from T1W sequences and pathologies (7). In this study, T1W sequences proved beneficial for discerning anatomical structures, and T2W was evaluated with higher reliability for application in patients. The PD sequence heightened the sig-
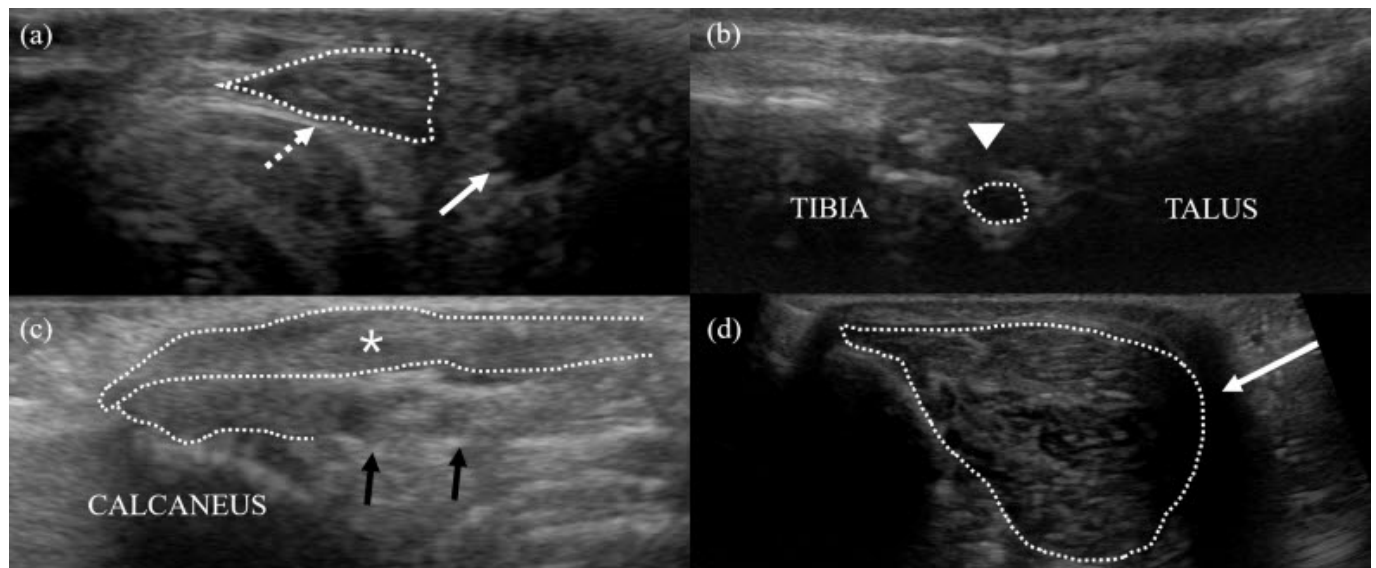

Fig. 4. Tarsal structures evaluated with ultrasound score above 3.0.; dashed arrow, tibialis cranialis tendon; short arrow, cranial tibial artery; arrowhead, joint space; asterisk, superficial digital flexor tendon; black arrow, deep digital flexor tendon; long arrow, cranial tibial muscle.

nal intensity for fluids, facilitating the assessment of fluid-surrounded structures such as narrow joint spaces, and serving as a useful sequence for distinguishing small structures from bones (7). In this study, while receiving lower score than in T2W and T1W, PD FS demonstrated an advantage for the evaluation of tendons and joint spaces with a scoring above 3.0. Moreover, fat saturation effectively suppressed the neighboring fat signal, resulting in enhanced clarity of structural evaluations.

In a previous study, sternal recumbency was primarily performed during tarsal MRI (7,10,17). While applying sternal recumbency in this study, the appropriate angles for both tarsi could not be determined. To address this, the patient was positioned in lateral recumbency and a sponge model was applied to immobilize both legs. However, aligning both tarsus joints in parallel is challenging, therefore each side is individually immobilized. During imaging of one tarsus, the opposite leg was extended forward and positioned outside the coil. In cases in which a comparison between both sides is crucial for the patient, maintaining a lateral position that allows for an appropriate angle is considered more suitable, and the use of an appropriate supportive device to ensure symmetry is necessary.

When performing ultrasound scans in a previous study, the dog was oriented in left lateral recumbency during right tarsus scans; conversely, for the left tarsus scans, the dog was positioned in right lateral recumbency (3). This approach facilitated more comfortable scanning of the dorsal, lateral, and plantar regions of the targeted tarsus, as it allowed the scanned tarsus to be elevated upward. To visualize the structures on the medial portion, the patient would need to be positioned in the opposite recumbency (3). However, unlike previous studies, a dorsal recumbent position was adopted when examining the dorsal and plantar portions of the tarsus. By maintaining the contact surface of the probe parallel to the ground during scanning, the tarsus was more easily visualized, and the examiner could conduct the examination in a more comfortable posture. To evaluate the medial and lateral portions, the lateral recumbency position was considered the most suitable position. Also, it is suggested that when examining the dorsal and plantar portions, the dorsal recumbency position should be chosen as per convenience.

When considering the evaluation scores of all the structures and planes in the MRI sequences, the average assessment score was 3.72 for the T1W images, 3.59 for T2W images, and 2.69 for PD FS images were calculated. When evaluating the tarsus with MRI, T1W imaging is considered the most useful sequence, and similarly, T2-weighted imaging is also deemed to have high evaluative utility. In the case of PD FS, although the average score is lower, the overall utility is presumed to be diminished due to restrictions in evaluating certain structures. The subsequent paragraphs delve into the evaluation of each structure and plane within each sequence.

When MRI was employed to evaluate bones, the transverse plane in all sequences was the most conducive for assessment. Subcutaneous fat was rated the highest in the T1W sagittal plane and in the T2W transverse and sagittal planes. The vascular structures were most easily assessed in the T1W sagittal plane. The cranial tibialis muscle in the T1W sagittal plane and the joint space in the dorsal and sagittal planes for both the T1W and T2W sequences were considered optimal conditions. Both the superficial and deep digital flexor tendons were assessed most favorably in the sagittal plane in both T1W and T2W sequences. Finally, the cranialis tibialis tendon was most useful in the T1W transverse plane, whereas it received scores under 3.0 in all other sequences and planes.

PD FS enhances the contrast of non-adipose soft tissue structures, selectively suppress fat signals, and aid in the evaluation of ligaments, bones, muscles, cartilage, and edema, particularly in musculoskeletal assessments for improved visualization (13). However, in this study, the utility scores for the musculoskeletal structures on PD FS were predominantly rated at ≤3.0. Among these, the evaluation utility scores for the deep and superficial digital flexor tendons, although considered somewhat useful in certain cross-sections, remained in the 3-point range. The relatively small size of the musculoskeletal structure composing the tarsus sets it apart, exhibiting differences compared with previous studies.

Overall, MRI is generally more favorable and easier to assess than ultrasound. However, for the cranial tibialis muscle and deep digital flexor tendon, a reasonably reliable assessment can be conducted. Additionally, other structures such as subcutaneous fat, joint space, and the superficial digital flexor tendon are considered to have moderate reliability but the potential for partial assessment. Therefore, for these specific structures, ultrasound can be considered an initial screening modality before MRI.

This study has several limitations. First, the evaluation was based on subjective assessment criteria and the lack of objective assessment metrics may have resulted in some degree of subjectivity. Second, not all MRI sequences were scanned, which limited the selection of the most favorable sequence for tarsal evaluation. Third, it remains challenging to compare MRI and ultrasound because of the differences in image cross-sections. Lastly, it should be noted that the applicability in small-sized dogs was not assessed.

In this study, ultrasound and MRI images of the tarsal struc-

tures were obtained and compared. In tarsus MRI imaging, the T1W was considered the most useful sequence. Although MRI is anticipated to be more beneficial for a comprehensive assessment of the entire structure, when comparing selectively imaged structures in ultrasound to their corresponding areas in MRI, ultrasound also appears capable of providing clinically useful substantive evaluations in cranial tibialis muscle, deep digital flexor tendon, subcutaneous fat, joint space, and the superficial digital flexor tendon. In addition, specific structures of interest can be evaluated using ultrasound sections, MRI sequences, and planes that offer optimal visibility of particular structures. In veterinary clinical practice, for pathologies in the tarsal region, an initial assessment using ultrasound can be conducted with optimal visibility and further evaluation of additional structures is deemed necessary, and MRI examinations with MRI sequences and planes that exhibit the highest evaluation utility can be pursued.

Conflicts of Interest

The authors have no conflicting interests.

References

1. Abako J, Holak P, Głodek J, Zhalniarovich Y. Usefulness of imaging techniques in the diagnosis of selected injuries and lesions of the canine tarsus. A review. Animals (Basel) 2021; 11: 1834.

2. Butler D, Nemanic S, Warnock JJ. Comparison of radiography and computed tomography to evaluate fractures of the canine tarsus. Vet Radiol Ultrasound 2018; 59: 43-53.

3. Caine A, Agthe P, Posch B, Herrtage M. Sonography of the soft tissue structures of the canine tarsus. Vet Radiol Ultrasound 2009; 50: 304-308.

4. Carlisle CH, Reynolds KM. Radiographic anatomy of the tarsocrural joint of the dog. J Small Anim Pract 1990; 31: 273-279.

5. Craig LE, Julian ME, Ferracone JD. The diagnosis and prognosis of synovial tumors in dogs: 35 cases. Vet Pathol 2002; 39: 66-73.

6. Daoualibi Y, Pohl CB, Kemper RT, Rolemberg KM, Demeulemeester SC, Bandinelli MB, et al. Tarsal villonodular tenosynovitis (giant cell tumor of tendon sheath) in a dog. Cienc Rural 2021; 51: e20200786.

7. Deruddere KJ, Milne ME, Wilson KM, Snelling SR. Magnetic resonance imaging, computed tomography, and gross anatomy of the canine tarsus. Vet Surg 2014; 43: 912-919.

8. Dik KJ. Ultrasonography of the equine tarsus. Vet Radiol Ultrasound 1993; 34: 36-43.

9. Dorfman SK, Hurvitz AI, Patnaik AK. Primary and secondary bone tumours in the dog. J Small Anim Pract 1977; 18: 313-326.

10. Fitch RB, Wilson ER, Hathcock JT, Montgomery RD. Radiographic, computed tomographic and magnetic resonance imaging evaluation of a chronic long digital extensor tendon avulsion in a dog. Vet Radiol Ultrasound 1997; 38: 177-181.

11. Gielen IM, De Rycke LM, van Bree HJ, Simoens PJ. Computed tomography of the tarsal joint in clinically normal dogs. Am J Vet Res 2001; 62: 1911-1915.

12. Harasen G. Arthrodesis--Part II: the tarsus. Can Vet J 2002; 43: 806-808.

13. Hodgson RJ, O'Connor PJ, Grainger AJ. Tendon and ligament imaging. Br J Radiol 2012; 85: 1157-1172.

14. Koo Y, Yun T, Chae Y, Lee D, Kim H, Yang MP, et al. Cutaneous angiomatosis in a dog: a case report. Korean J Vet Res 2021; 61: e28.

15. Lamb CR, Duvernois A. Ultrasonographic anatomy of the normal canine calcaneal tendon. Vet Radiol Ultrasound 2005; 46: 326-330.

16. Levine BD, Motamedi K, Seeger LL. Imaging of the shoulder: a comparison of MRI and ultrasound. Curr Sports Med Rep 2012; 11: 239-243.

17. Lin M, Glass EN, Kent M. Utility of MRI for evaluation of a common calcaneal tendon rupture in a dog: case report. Front Vet Sci 2020; 7: 602.

18. Liuti T, Saunders JH, Gielen I, De Rycke L, Coopman F, van Bree H. Ultrasound approach to the canine distal tibia and trochlear ridges of the talus. Vet Radiol Ultrasound 2007; 48: 361-367.

19. Maher MA, Emam IA. Normal vascular and nerve distribution of the pes region in dogs: an anatomical and diagnostic imaging. Int J Vet Sci 2020; 9: 259-266.

20. Morgan JP, Wind A, Davidson AP. Bone dysplasias in the labrador retriever: a radiographic study. J Am Anim Hosp Assoc 1999; 35: 332-340.

21. Nordberg CC, Johnson KA. Magnetic resonance imaging of normal canine carpal ligaments. Vet Radiol Ultrasound 1999; 40: 128-136.

22. Perinetti G. StaTips Part IV: selection, interpretation and reporting of the intraclass correlation coefficient. South Eur J Orthod Dentofac Res 2018; 5: 3-5.

23. Roch SP, Clements DN, Mitchell RA, Downes C, Gemmill TJ, Macias C, et al. Complications following tarsal arthrodesis using bone plate fixation in dogs. J Small Anim Pract 2008; 49: 117-126.

24. Rosenblum GP, Robins GM, Carlisle CH. Osteochondritis dissecans of the tibio-tarsal joint in the dog. J Small Anim Pract 1978; 19: 759-767.

25. Sabiza S, Khajeh A, Naddaf H. Reconstruction of long digital extensor tendon by cranial tibial muscle fascia graft in a dog. Vet Res Forum 2016; 7: 271-274.

26. Sjöström L, Håkanson N. Traumatic injuries associated with the short lateral collateral ligaments of the talocrural joint of the dog. J Small Anim Pract 1994; 35: 163-168.

27. Stahl C, Wacker C, Weber U, Forterre F, Hecht P, Lang J, et al. MRI features of gastrocnemius musculotendinopathy in herding dogs. Vet Radiol Ultrasound 2010; 51: 380-385.

28. Sullivan CV, Zuckerman J, Popovitch C. Caudal thigh intermuscular lipomas in dogs: anatomic review and approach to surgical excision. Can Vet J 2021; 62: 1219-1224.

29. Vaughan LC. Disorders of the tarsus in the dog. I. Br Vet J 1987; 143: 388-401.